Characterization of an Intermediate in the Reduction of Acetylene by the Nitrogenase α-Gln^{195} MoFe Protein by Q-band EPR and ^{13}C,^{1}H ENDOR

Hong-In Lee,[†] Morten Sørlie,[‡] Jason Christiansen,[§] Ruitian Song,[†] Dennis R. Dean,*[,§] Brian J. Hales,*[,‡] and Brian M. Hoffman*[,†]

Contribution from the Department of Chemistry, Northwestern University, Evanston, Illinois 60208, Department of Chemistry, Louisiana State University, Baton Rouge, Louisiana 70803, and Department of Biochemistry, Virginia Tech, Blacksburg, Virginia 24061

Received February 14, 2000. Revised Manuscript Received April 18, 2000

Abstract: Recent X-band EPR investigations of an altered nitrogenase MoFe protein for which the α-subunit His^{195} residue has been substituted by Gln(α-Gln^{195} MoFe protein) revealed that it exhibits three new $S = {}^1/_2$ EPR signals when incubated under turnover conditions in the presence of acetylene (C_2H_2). These three signals are designated S_{EPR1}, S_{EPR2}, and S_{EPR3}. We now report Q-band EPR and ^{13}C and ^{1}H ENDOR of the α-Gln^{195} MoFe protein when incubated under turnover conditions in either H_2O or D_2O buffers with $^{12}C_2H_2$, $^{13}C_2H_2$, or C_2D_2 as the substrate. ENDOR measurements from S_{EPR1} prepared with $^{13}C_2H_2$ reveal interactions with three distinct ^{13}C nuclei, indicating that at least two C_2H_2-derived species are bound to the cofactor of the α-Gln^{195} MoFe protein under turnover conditions. Although distinct, two of these species have approximately isotropic hyperfine tensors, with hyperfine splittings of A(C1,C2) ∼ 2.4 MHz; the third has a smaller hyperfine splitting, A(C3) ≤ 0.5 MHz at g_1. ^{1}H ENDOR measurements further show strongly coupled proton signals (A ∼ 12 MHz) that are associated with bound C_2H_x. The observation of this signal from the C_2H_2/D_2O sample indicates that this proton is not exchangeable with solvent in this cluster-bound state. Conversely, the absence of a signal in the C_2D_2/H_2O sample indicates that there is no strongly coupled proton derived from solvent. We propose that we are monitoring a C_2H_2 species that is bound to the FeMo-cofactor by bridging two Fe ions of a 4Fe4S "face", thereby stabilizing the $S = {}^1/_2$ cluster state. Q-band EPR also resolves rhombic features in the spectrum of S_{EPR2}, giving g = [2.007, 2.000, 1.992], but ENDOR showed no ^{13}C signals with enriched substrate, confirming an earlier suggestion that this signal is not derived from C_2H_2.

Nitrogenase, the catalytic component of biological nitrogen fixation, is comprised of the MoFe protein and the Fe protein. During catalysis the Fe protein serves as a MgATP-dependent reductant of the MoFe protein, which provides the site for substrate binding and reduction.[1] The MoFe protein contains two metal centers of biologically unique structure, the P-cluster (Fe_8-S_7) and the FeMo-cofactor (Fe_7S_9Mo:homocitrate).[2] There is compelling biochemical, spectroscopic, and genetic evidence that substrate binding and reduction occurs at the FeMo-cofactor site (for a review, see ref 3). In addition to dinitrogen, nitrogenase also reduces other small molecules with multiple bonds, such as C_2H_2, HCN, N_3^-, and CS_2.[4,5]

Although X-ray crystallographic modeling has revealed the organization and the architecture of the FeMo-cofactor, as well as its peptide surroundings,[2] the molecular details of the interaction between substrates and FeMo-cofactor remain uncertain. Recently, the interaction between FeMo-cofactor and CO, a small-molecule inhibitor of all nitrogenase substrate reduction activities except proton reduction, was studied by using electron−nuclear double resonance spectroscopy (ENDOR) under conditions of enzymatic turnover.[6−9] These studies showed that one CO molecule is bound to the FeMo-cofactor at low pressure (P_{CO} = 0.08 atm, responsible for the so-called lo-CO EPR signal) and that two CO molecules are bound at high pressure (P_{CO} = 0.5 atm, responsible for the so-called hi-CO EPR signal).[8] This work also provided the first experimental characterization of the FeMo-cofactor metal-ion valencies and put forth proposals for the binding modes of CO.[6,7] In contrast, investigation of the interaction of the FeMo-cofactor with substrates has proven more difficult. The main reason for this difficulty is that, until recently,[10,11] there have been no significant spectroscopic signatures associated with a substrate-bound form of the enzyme.

[†] Northwestern University.
[‡] Louisiana State University.
[§] Virginia Tech.

(1) Burgess, B. K.; Lowe, D. L. *Chem. Rev.* **1996**, *96*, 2983−3011.
(2) Howard, J. B.; Rees, D. C. *Chem. Rev.* **1996**, *96*, 2965−2982.
(3) Dean, D. R.; Bolin, J. T.; Zheng, L. *J. Bacteriology* **1993**, *175*, 6737−6744.
(4) Burris, R. H. *J. Biol. Chem.* **1991**, *266*, 9339−9342.
(5) Seefeldt, L. C.; Rasche, M. E.; Ensign, S. A. *Biochemistry* **1995**, *34*, 5382−5389.
(6) Lee, H.-I.; Hales, B. J.; Hoffman, B. M. *J. Am. Chem. Soc.* **1997**, *119*, 11395−11400.
(7) Lee, H.-I.; Cameron, L. M.; Hales, B. J.; Hoffman, B. J. *J. Am. Chem. Soc.* **1997**, *119*, 10121−10126.
(8) Pollock, R. C.; Lee, H.-I.; Cameron, L. M.; DeRose, V. J.; Hales, B. J.; Orme-Johnson, W. H.; Hoffman, B. M. *J. Am. Chem. Soc.* **1995**, *117*, 8686−8687.
(9) Christie, P. D.; Lee, H.-I.; Cameron, L. M.; Hales, B. J.; Orme-Johnson, W. H.; Hoffman, B. M. *J. Am. Chem. Soc.* **1996**, *118*, 8707−8709.
(10) Sørlie, M.; Christiansen, J.; Dean, D. R.; Hales, B. J. *J. Am. Chem. Soc.* **1999**, *121*, 9457−9458.
(11) Ryle, M. J.; Lee, H.-I.; Seefeldt, L. C.; Hoffman, B. M. *Biochemistry* **2000**, *39*, 1114−1119.

10.1021/ja000542g CCC: $19.00
Published on Web 05/26/2000

One notable exception has been the Q-band EPR study of the interaction of CS_2 with the FeMo-cofactor, which was able to described three separate signals.[11] Temporal freeze-quench experiments further indicated that each of these signals could be assigned to a different reaction intermediate in the pathway of CS_2 reduction. ^{13}C ENDOR was then used to characterize the interaction of these intermediates with the FeMo-cofactor and give insights into the binding of CS_2 to the nitrogenase active site.[11]

Of all nitrogenase substrates, C_2H_2 is the best-studied, and its reduction to ethylene (C_2H_4) is routinely used for in vitro assays of nitrogenase activity.[4] Despite the many models that have been suggested for C_2H_2 binding to the FeMo-cofactor,[12] until recently there has been no direct spectroscopic observation of C_2H_2 interaction with the nitrogenase FeMo-cofactor. When wild-type nitrogenase is incubated under turnover conditions there is a dramatic reduction in the intensity of the $S = {}^3/_2$ EPR signal associated with the resting state of FeMo-cofactor. However, this situation does not result in the appearance of other paramagnetic species that can be correlated with the binding of substrates such as N_2 or C_2H_2. By using an altered MoFe protein for which the α-subunit His[195] residue was substituted by Gln (designated α-Gln[195] MoFe protein) we recently detected the first EPR signals that are elicited by the binding of C_2H_2 to the FeMo-cofactor under turnover conditions.[10] The α-Gln[195] MoFe protein does not significantly reduce N_2 but remains capable of reducing C_2H_2 and does so with kinetic parameters very similar to the wild-type enzyme.[13] When incubated under turnover conditions in the presence of C_2H_2, the α-Gln[195] MoFe protein exhibits three simultaneously generated EPR signals: a rhombic $g = [2.12, 1.98, 1.95]$ signal (designated S_{EPR1}); a mostly isotropic, $g = 2.00$ signal (designated S_{EPR2}); and a minority component with an inflection at $g \sim 1.97$ (designated S_{EPR3}). The spectrum obtained by using isotopically labeled $^{13}C_2H_2$ indicated that S_{EPR1} originates from C_2H_2 intermediates bound to the FeMo-cofactor during enzymatic turnover, while the EPR signal of S_{EPR2} is most likely associated with an amino acid or homocitrate radical species generated during turnover. In this report, we present the first direct evidence regarding the mode of binding of an C_2H_2 reduction intermediate to the FeMo-cofactor, as obtained through Q-band ^{13}C and ^1H (proton) ENDOR spectroscopy of the nitrogenase S_{EPR1} turnover state.

Materials and Methods

Cell Growth and Protein Purification. The α-Gln[195] MoFe protein was purified from *Azotobacter vinelandii* strain DJ997. Cells were grown at 30 °C with pressurized sparging (80 L/min at 5 psi) and 125 rpm agitation in a 150-L custom-built fermenter (W. B. Moore, Inc. Easton, PA) in modified Burk medium containing 10 mM urea as the sole nitrogen source.[14] After reaching a density of 220 Klett units (red filter), the cells were derepressed for *nif* gene expression by concentration (6-fold) using a custom-built AG Technologies tangential-flow concentrator and resuspended in Burk medium with no added nitrogen. All protein manipulations were performed under anaerobic conditions maintained using either a Schlenk apparatus[15] or an anaerobic glovebox. The α-Gln[195] MoFe protein was purified using a combination of immobilized metal-affinity chromatography (IMAC) and DEAE-Sepharose anion exchange chromatography as previously described.[16] Protein was quantified using a modified biuret assay with bovine serum albumin as the standard[17] and purity was monitored by SDS-PAGE electrophoresis.[18] For 360 g of wet-weight cells, purification yielded approximately 1.1 g of purified α-Gln[195] MoFe protein. Nitrogenase assays were performed as previously described[19,20] and activities for the α-Gln[195] MoFe protein used in the current work were similar to those previously reported.[19]

Turnover EPR Samples. Turnover samples consisted of 20 μM Fe protein, 100 μM α-Gln[195] MoFe protein, 0.1 atm of C_2H_2, 10 mM ATP, 25 mM $MgCl_2$, 20 mM $Na_2S_2O_4$, and 38 mM TES-KOH at pH 7.4. Prior to turnover, the above mixture (without the Fe protein) was preincubated for 20 min at 30 °C with 0.1 atm of the appropriate experimental gas (i.e. C_2H_2, C_2D_2, etc.) under 1.0 atm of Ar. After initiation of turnover by the addition of Fe protein, a 100 μL sample was transferred to a Q-band ENDOR tube where it was rapidly frozen in liquid N_2. The interval between turnover initiation and final freezing was approximately 2 min. For experiments performed in D_2O, protein was first exchanged into buffered D_2O (initally 99.8% in 38 mM TES-KOD at pD 7.4) to yield a final solution of about 95% D_2O. The ATP regenerating solution for these experiments was prepared in 99.8% D_2O for a final concentration (including protein) in the turnover mixture of about 98% D_2O.

EPR and ENDOR Spectroscopy. EPR and ENDOR spectra were recorded on a modified Varian E-110 spectrometer equipped with a helium immersion dewar. The spectra were obtained in dispersion mode using 100 kHz field modulation under "rapid passage" conditions.[21−23] Spectra shown represent the absorption spectrum, not the derivative. For ENDOR, the bandwidth of radio frequency (RF) was broadened to 100 kHz to improve the signal-to-noise ratio.[24]

For a single orientation of a paramagnetic center, the first-order ENDOR spectrum of a nucleus with $I = {}^1/_2$ in a single paramagnetic center consists of a doublet with frequencies given by:[25]

$$\nu_{\pm} = |\nu_N \pm A/2| \quad (1)$$

Here, ν_N is the nuclear Larmor frequency and A is the orientation-dependent hyperfine coupling constant of the coupled nucleus. The doublet is centered at the Larmor frequency and separated by A when $\nu_N > |A/2|$, as is the case for both ^{13}C and ^1H spectra observed here. The full hyperfine tensor of a coupled nucleus can be obtained by analyzing a "2-D" set of ENDOR spectra collected across the EPR envelope, as described elsewhere.[26−30]

(12) Henderson, R. A. *Angew. Chem., Int. Ed. Engl.h* **1996**, *35*, 947−967.
(13) Kim, C.-H.; Newton, W. E.; Dean, D. R. *Biochemistry* **1995**, *34*, 2798−2808.
(14) Scott, D. J.; Dean, D. R.; Newton, W. E. *J. Biol. Chem* **1992**, *267*, 20002−20010.
(15) Burgess, B. K.; Jacobs, D. B.; Stiefel, E. I. *Biochim. Biophys. Acta* **1980**, *614*, 196−209.
(16) Christiansen, J.; Goodwin, P. J.; Lanzilotta, W. N.; Seefeldt, L. C.; Dean, D. R. *Biochemistry* **1998**, *37*, 12611−23.
(17) Chromy, V.; Fischer, J.; Kulhanek, V. *Clin. Chem.* **1974**, *20*, 1362−1363.
(18) Laemmli, U. K. *Nature* **1970**, *227*, 680−685.
(19) Kim, C.-H.; Zheng, L.; Newton, W. E.; Dean, D. R. In *New horizons in nitrogen fixation*; Palacios, R., Mora, J., Newton, W. E., Eds.; Kluwer Academic Publishers: Norwell, MA 1992; pp 105−110.
(20) Peters, J. W.; Fisher, K.; Dean, D. R. *J. Biol. Chem.* **1994**, *269*, 28076−28083.
(21) Werst, M. M.; Davoust, C. E.; Hoffman, B. M. *J. Am. Chem. Soc.* **1991**, *113*, 1533−1538.
(22) Mailer, C.; Taylor, C. P. S. *Biochim. Biophys. Acta* **1973**, *322*, 195−203.
(23) Feher, G. *Phys. Rev.* **1959**, *114*, 1219−1244.
(24) Hoffman, B. M.; DeRose, V. J.; Ong, J. L.; Davoust, C. E. *J. Magn. Reson.* **1994**, *110*, 52−57.
(25) Abragam, A.; Bleaney, B. *Electron Paramagnetic Resonance of Transition Metal Ions*, 2nd ed.; Clarendon Press: Oxford, 1970.
(26) Hoffman, B. M. *Acc. Chem. Res.* **1991**, *24*, 164−170.
(27) Hoffman, B. M.; DeRose, V. J.; Doan, P. E.; Gurbiel, R. J.; Houseman, A. L. P.; Telser, J. In *Biological Magnet Resonance*; Berliner, L. J., Reuben, J., Eds.; Plenum Press: New York and London 1993; Vol. 13, pp 151−218.
(28) Hoffman, B. M.; Gurbiel, R. J.; Werst, M. M.; Sivaraja, M. In *Advanced EPR*; Hoff, A. J., Ed.; Elsevier: Amsterdam, 1989.
(29) Hoffman, B. M.; Martinsen, J.; Venters, R. A. *J. Magn. Reson.* **1984**, *59*, 110−123.
(30) Hoffman, B. M.; Venters, R. A.; Martinsen, J. *J. Magn. Reson.* **1985**, *62*, 537−542.

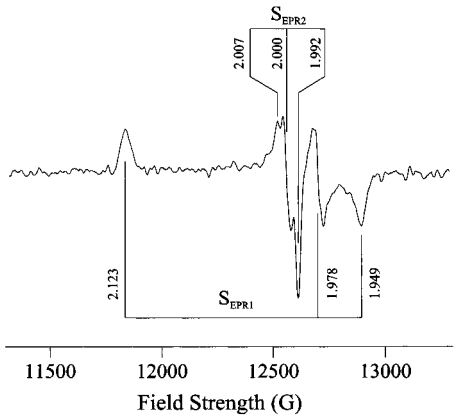

Figure 1. Q-band EPR spectrum for a turnover sample of the α-Gln[195] MoFe protein in the presence of C_2H_2 (0.1 atm). The *g*-factors of S_{EPR1} and S_{EPR2} are depicted in the figure. Experimental conditions: [Fe protein]/[α-Gln[195] MoFe protein] = [0.020 mM]/[0.100 mM; [C_2H_2] = 0.1 atm; [ATP] = 10 mM; [$MgCl_2$] = 25 mM; [$Na_2S_2O_4$] = 20 mM; 50 mM TES-KOH, pH 7.4. The sample was rapidly frozen in liquid N_2 3 min following the initiation of turnover. EPR and ENDOR (Figure 2) spectra were obtained at 2 K in dispersion mode using 100 kHz field modulation. Under these "rapid passage" conditions, actual experimental data represent the absorption envelope. The spectrum presented here is the numerical derivative of the experimental data. Spectrometer conditions: microwave frequency, 35.160 GHz; modulation amplitude, 1.3 G.

Results

EPR Spectra. Figure 1 shows the Q-band (35 GHz) EPR spectrum of the α-Gln[195] MoFe protein under turnover conditions in the presence of C_2H_2. While the Q-band spectrum yields greater resolution than seen previously at X-band, the *g*-factors of S_{EPR1} are in agreement with the X-band EPR result.[10] However, rhombicity in the **g**-tensor for S_{EPR2} was not well resolved at X-band, but is clearly seen at Q-band, with **g** = [2.007, 2.00, 1.992]. In contrast, the spectrum of the minor S_{EPR3} species is not reliably observed at Q-band. A penalty paid for the use of higher microwave frequencies is that they enhance the EPR signals from adventitious Mn^{2+}. The ENDOR samples exhibited such signals in low intensity, but this is significant because Mn^{2+} exhibits strong ^{1}H ENDOR signals from bound water,[31] and even the minimal amount of Mn^{2+} in our samples precluded reliable detection of ^{1}H signals from S_{EPR1} at fields above $g \sim 2.04$ (fields above ~12 300 G, see below).

^{13}C ENDOR Data. Figure 2 shows Q-band ^{13}C ENDOR collected at fields across the EPR envelope of S_{EPR1} generated during turnover of a α-Gln[195] MoFe protein sample in the presence of $^{13}C_2H_2$. The presence of one or more fragments arising from $^{13}C_2H_2$ bound to the EPR-active FeMo-cofactor is indicated by the ^{13}C signals associated with S_{EPR1} that are absent in the ENDOR spectrum of the sample prepared with natural abundance C_2H_2. In contrast, ENDOR spectra taken near $g = 2.0$, at magnetic field positions where S_{EPR2} is present, did not exhibit ^{13}C signals, supporting the previous suggestion that S_{EPR2} is not a C_2H_2 adduct radical.[10]

The top ^{13}C ENDOR spectrum in Figure 2 was obtained at the low-field edge of the S_{EPR1} ($g_1 = 2.12$) spectrum. This spectrum represents a "single-crystal-like" pattern associated with a single molecular orientation, with the magnetic field along g_1. In such a spectrum, each ^{13}C ENDOR doublet is associated with a single class of nuclei. Signals from three such classes

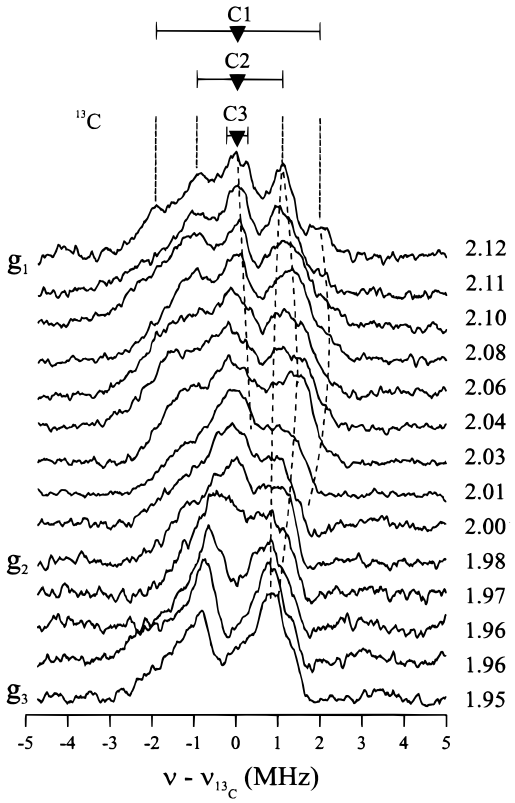

Figure 2. Q-band ^{13}C ENDOR spectra for the S_{EPR1} signal arising from the α-Gln[195] MoFe protein during turnover in the presence of $^{13}C_2H_2$ (0.1 atm). Spectra were taken at *g*-values across the EPR envelope of S_{EPR1}, as indicated. The spectra are centered at the ^{13}C Larmor frequency. The three ^{13}C doublets detected in the single-crystal-like spectrum at g_1 are indicated. The development of these spectra with field, insofar as they can be traced clearly, is indicated by the dashed lines overlaid to guide the eye on the ν^+ branch of the spectra. As is common in Q-band spectra, the ν^- branch is less resolved and so the corresponding lines are not included. Conditions: microwave frequency, 35.158 GHz; modulation amplitude, 1.3 G; radio frequency (RF) power, 20 W. The bandwidth of RF was broadened to 100 kHz.

can be recognized. Two of these yield well-resolved doublets, with coupling constants A(C1) = 3.9 MHz and A(C2) = 2.0 MHz. The ENDOR intensity near the ^{13}C Larmor frequency, although not resolved into a doublet, nonetheless must originate from a third type of weakly coupled ^{13}C nucleus, with A(C3) ≤ 0.5 MHz. This spectrum therefore requires the presence of no fewer than two molecules of C_2H_2, or its reaction intermediates/products, bound to the S_{EPR1} FeMo-cofactor. This conclusion is consistent with the cooperativity that is associated with the production of the EPR signal at X-band frequencies.[10]

The strong overlap of the signals from the three types of ^{13}C nucleus prevents an accurate determination of their hyperfine tensors. However, the 2-D, field-frequency pattern of Figure 2 can nonetheless be analyzed approximately. As indicated in the figure, the field-dependence of the ν^+ branch of the pattern for C2 can be reasonably well followed. The modest change in hyperfine coupling with field is characteristic of a nucleus with a largely isotropic coupling, and the nature of the change indicates the anisotropic term is of roughly axial symmetry.[26−30] The tensor appears to be roughly coaxial, having a **g**-tensor with principal values of ca. **A**(C2) ~ [3.2, 2, 1.8] MHz, corresponding to an isotropic contribution, a(C2) ~ 2.3 MHz, and anisotropic term, $2T$(C1) ~ 0.9 MHz.

The coupling to C1 at g_1 is A(C1) ~ 3.6 MHz, significantly greater than that of C2, but the C1 coupling is more anisotropic

(31) Tan, X. L.; Bernardo, M.; Thomann, H.; Scholes, C. P. *J. Chem. Phys.* **1993**, *98*, 5147−5157.

and decreases with increasing field until the C1 signal becomes undistinguishable as g approaches g_2 (Figure 2). If, for heuristic purposes, we assume that C1 contributes, together with C2, to the intense doublet seen at g_3 ($A \sim 2$ MHz), then the 2-D pattern can be roughly described by a hyperfine tensor with principal values of, **A**(C1) $\sim$ [3.8, 1.8, 1.8] MHz, rotated from the **g**-tensor frame about g_2, corresponding to an isotropic contribution, a(C1) $\sim$ 2.5 MHz, and anisotropic term, $2T$(C1) $\sim$ 1.4 MHz. Thus, the hyperfine tensors of both C1 and C2 appear to be dominated by isotropic hyperfine couplings of comparable magnitude, but with a larger anisotropic term for C1.

As indicated in Figure 2, the weak coupling to C3 increases somewhat as the field is increased from g_1 to $g \sim 2.027$. It is impossible to determine whether the coupling continues to increase beyond this point, perhaps even reaching $A \sim 2$ MHz at g_3, or whether it decreases to the extent that it becomes unobservably small at g_3.

^{1,2}H Endor Data. To characterize the protonation state of the C_2H_2-derived species bound to the EPR-active turnover FeMo-cofactor, we prepared turnover samples with C_2H_2 in H_2O and in D_2O buffers, and with C_2D_2 in the same buffers. Figure 3A presents ^{1}H endor spectra of the four samples, taken at $g = 2.084$. In addition to the intense, unresolved feature from weakly coupled protons, seen near ν_H in both spectra, there is a broad pattern from strongly coupled doublet protons in both the C_2H_2/H_2O and D_2O samples, with maximum coupling of A_{max}(H) $\sim$ 13 MHz, that is absent in the C_2D_2 samples prepared in either H_2O or D_2O.

The most dramatic observation is the loss of the strongly coupled proton signal seen for samples prepared with C_2H_2 prepared by turnover of C_2D_2 in H_2O buffer. This clearly demonstrates that the signal must be associated with a C−H of an acetylene-derived fragment that is bound to the turnover cluster, and that this proton is not exchangeable with solvent in its cluster-bound state. Conversely, the absence of the signal means that there is *no* strongly coupled exchangeable proton derived from solvent.

Additional spectra have been taken at fields between 1.188 ($g \sim g_1$) and 1.237 T ($g \sim 2.03$), Figure 3B. These show that the signal from the strongly coupled proton has a maximum coupling at 1.188 T of A(H) $\sim$ 11 MHz, but $\sim$18 MHz at 1.237 T. This indicates that the hyperfine interaction has a large isotropic component, probably no less that $\sim$13 MHz, and also substantial anisotropy, totalling no less than $\sim$7 MHz. Unfortunately, the spectrum of this proton (or protons) cannot be followed across the entire EPR envelope, so as to allow a full determination of the hyperfine tensor; at higher fields, low levels of aquo-Mn^{2+} impurities give proton signals that overlap and could not be eliminated reliably by D_2O exchange, given the low concentration of the nitrogenase turnover species. However, the field dependence in the figure does indicate that the interaction is appreciably isotropic in character, as expected for spin delocalization onto an acetylene-derived species datively bonded to the FeMo-cofactor. The inability to perform a full analysis, however, precludes the use of these data to determine the number of protons that contribute to this strongly coupled signal.

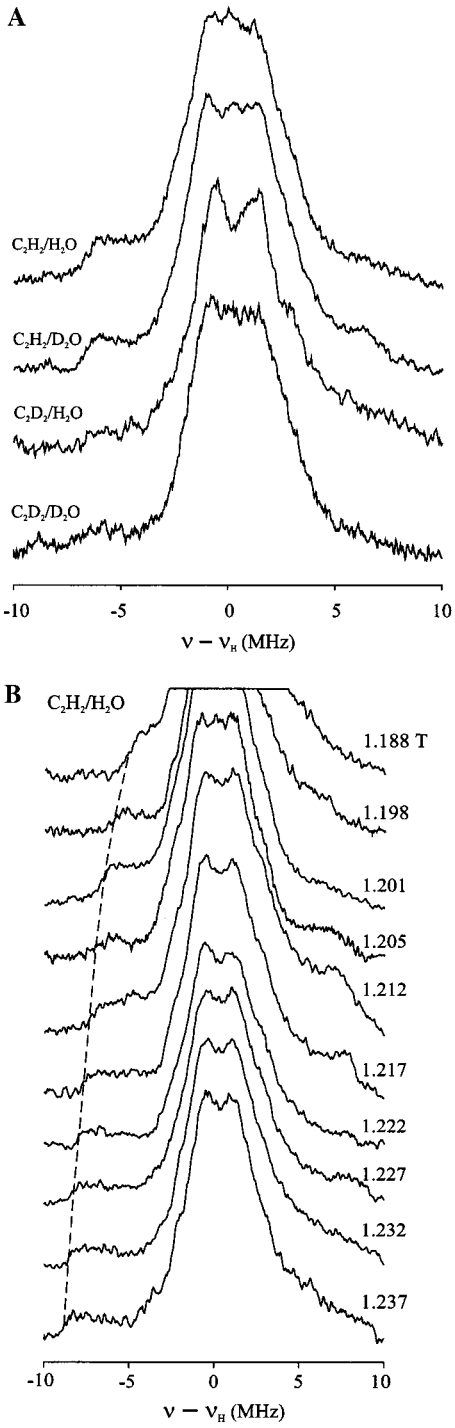

Figure 3. (A) ^{1}H ENDOR spectra of nitrogenase under turnover conditions with C_2H_2 and C_2D_2 in H_2O and in D_2O buffers (as indicated) at $g = 2.084$, showing the presence of a broad proton signal associated with C_2H_2 or a reaction fragment. Conditions: microwave frequencies were all in the range of 35.05 ± 0.01 GHz; modulation amplitude, 4 G; radio frequency (RF) power, 25 W; temperature, 2 K. (B) ^{1}H ENDOR spectra of nitrogenase under C_2H_2/H_2O turnover, collected at indicated fields. The dashed line indicates the extreme low-frequency edge of the patterns, and is included to guide the eye. Conditions: as above, except modulation amplitude was from 4 to 6.3 G to optimize the signal for different fields; radio frequency (RF) power was optimized at each field.

Discussion

The present study uses ^{13}C ENDOR to identify signals from three distinct, C_2H_2-derived ^{13}C nuclei that are bound to an EPR-active FeMo-cofactor that gives rise to the S_{EPR1} species observed for the α-Gln^{195} MoFe protein. Given that the FeMo-cofactor is the site of C_2H_2 reduction, and that our earlier work showed that CO binds to this EPR-active site during enzymatic turnover,[6−8] these three signals can be assigned to at least two C_2H_2-derived molecules that are interacting with the FeMo-cofactor. This conclusion is in line with other results that indicate

Table 1. ^{13}C Hyperfine Tensors of ^{13}C-Labeled Intermediates Bound to the FeMo-Cofactor of the Nitrogenase MoFe Proteins under Turnover Conditions in the Presence of Substrates/Inhibitors.

substrate/inhibitor	protein	EPR	**g**-tensor	^{13}C hyperfine couplings		ref
				tensor (MHz)	*a*(iso)	
CO	wild type	lo-CO	2.09, 1.97, 1.93	−2.0, 3.5, 2.0	3.2	
		hi-CO	2.17, 2.06, 2.06	5.8, 5.8, 4.5 (C1)	5.4	7
				0.6, 0.6, 0.9 (C2)	0.7	
CS_2	wild type	a	2.035, 1.982, 1.973		4.9[a]	
		b	2.111, 2.022, 1.956		1.8[a]	11
		c	2.211, 1.996, 1.978		2.7[a]	
C_2H_2	α-Gln^{195}	S_{EPR1}	2.12, 1.98, 1.95	3.8, 1.8, 1.8 (C1)	2.5	
				3.2, 2.0, 1.8(C2)	2.3	this work
				<0.5 (C3)		
		S_{EPR2}	2.007, 2.000, 1.992	*b*		
		S_{EPR3}	~1.97	*b*		

[a] Mostly isotropic hyperfine coupling tensor. [b] No bound substrates or reaction intermediates/products are observed in the ENDOR.

the presence of multiple C_2H_2 binding sites within the MoFe protein.[32−34] There are also signals arising from rather strongly coupled protons that are derived from C_2H_2 that are not exchangeable with solvent. Finally, there are no strongly coupled signals that arise from a solvent proton.

The C_2H_2-derived signals described here are not observed with the wild type MoFe protein, even though the wild type and α-Gln^{195} MoFe protein both exhibit nearly the same K_m values for C_2H_2 reduction. Both MoFe protein types also exhibit a comparable loss of the resting state $S = {}^3/_2$ EPR signal when placed under turnover conditions. One plausible qualitative explanation for the presence of a C_2H_2-induced, turnover-EPR signal in the case of the α-Gln^{195} MoFe protein is that the product release by the state giving rise to this signal is significantly slower than that for the wild-type MoFe protein. This situation could lead to a sufficient buildup of a population of an intermediate state that is observable by EPR. In contrast, the steady-state concentration of this species probably does not become sufficiently populated in the wild type MoFe protein such that it can be readily detected by EPR.

The data presented here can be used to consider possible binding mode(s) for the C_2H_2-derived species. Because C_2H_4 is the only detectable product of C_2H_2 reduction for both the wild type and α-Gln^{195} MoFe protein, we conclude that the ^{13}C and proton ENDOR we measure arises from cluster-bound C_2H_x species. The ^{13}C ENDOR hyperfine coupling tensors estimated for the S_{EPR1}-associated C_2H_x species are summarized in Table 1. Previous orientation-selective ^{13}C ENDOR experiments of CO-inhibited MoFe protein[7] and of the MoFe protein incubated under turnover conditions in the presence of $^{13}CS_2$[11] yielded the ^{13}C hyperfine coupling tensors of bound inhibitor and CS_2-related species (Table 1). The hyperfine interactions of C1 and C2 for S_{EPR1} are comparable to those previously reported for hi-^{13}CO (C1) and $^{13}CS_2$ adducts in that the tensors are mostly isotropic, with similar magnitudes for the isotropic couplings (Table 1). In these previous cases, we interpreted this type of ^{13}C hyperfine interaction as arising from terminally bound ^{13}C compounds. For this current discussion, we likewise assign C1 and C2 of S_{EPR1} to acetylene bound terminally to the cofactor. Such binding can occur either with coordination by a single carbon or by both carbons in a bridging arrangement with two Fe atoms, Figure 4A.

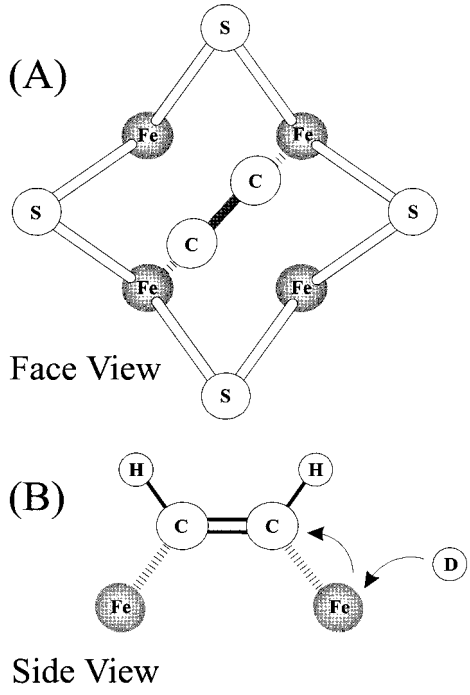

Figure 4. Sketches of the proposed binding mode for acetylene bound to the FeMo-cofactor of nitrogenase under turnover. (A) "Facial" bridging mode for binding of the C_2 fragment. (B) Binding of C_2H_2, including a cartoon of the pathway for addition of a deuterium during reduction.

The "Face View" of Figure 4A depicts one face of the waist region of the cofactor. EXAFS[35,36] and crystallographic[37] data have shown that the adjacent Fe−Fe distances are ca. 2.5−2.6 Å and diagonal, cross-face, Fe−Fe distances are ca. 3.6−3.8 Å. A simple energy minimization of one model (side view) gave an Fe−Fe distance of 3.9 Å.[38] Considering the potential flexibility of the FeMo-cofactor, this model appears acceptable.

(32) Davis, L. C.; Henzl, M. T.; Burris, R. H.; Orme-Johnson, W. H. *Biochemistry* **1979**, *18*, 4860−4869.

(33) Shen, J.; Dean, D. R.; Newton, W. E. *Biochemistry* **1997**, *36*, 4884−4894.

(34) Lowe, D. J.; Eady, R. R.; Thorneley, R. N. F. *Biochem. J.* **1978**, *173*, 277−290.

(35) Christiansen, J.; Tittsworth, R. C.; Hales, B. J.; Cramer, S. P. *J. Am. Chem. Soc.* **1995**, *117*, 10017−10024.

(36) Chen, J.; Christiansen, J.; Tittsworth, R. C.; Hales, B. J.; George, S. J.; Coucouvanis, D.; Cramer, S. P. *J. Am. Chem. Soc.* **1993**, *115*, 5509−5515.

(37) Peters, J. W.; Stowell, M. H. B.; Soltis, S. M.; Finnegan, M. G.; Johnson, M. K.; Rees, D. C. *Biochemistry* **1997**, *36*, 1181−1187.

(38) MM2 energy minimization was performed by using the molecular modeling and analysis program "CS Chem3D" (Cambridge Soft Co.: Cambridge, MA). The program employs Allinger's MM2 force field for energy minimization [Burkert, U.; Allinger, N. L. *Molecular Mechanics*; American Chemical Society; Washington, DC, 1982. Clark, T. C. *Computational Chemistry*; Wiley: New York, 1985]. In modeling the structure of the side view of Figure 4A (ii), *cis*-$(SH)_3FeCH{=}HCFe(SH)_3$ was constructed and the local geometry of each Fe ion was initially set to be tetrahedral.

However, acetylene has been shown to bind to, and bridge, transition metal atoms in a wide variety of different geometries, thus making this only one of many possibilities that could be consistent with the data presented here. Indeed, a recent study of a C_2H_2-resistant nitrogenase was interpreted to indicate that two C_2H_2 molecules are most likely bound and reduced at a single FeMo-cofactor 4Fe4S face.[39]

At first glance, it would appear that one must consider separately the possibilities that C1 and C2 are associated with the same C_2H_x fragment, or that each represents a bound carbon from a separate fragment. There are many scenarios, depending on the spin-coupling scheme of the cluster[6] and whether one considers single-point or bridging modes of attachment. However, any interaction with the cluster that gives rise to appreciable coupling to one carbon likely would give rise to a coupling of comparable magnitude to the other. For example, the spin of the C_2H_3 vinyl radical, which is to first approximation localized in a σ orbital on one carbon, gives rise to *larger* hyperfine couplings to the two protons on the other carbon than to the single proton on the "spin-bearing" carbon.[40,41] Hence we suggest that C1 and C2 are associated with the same C_2H_x fragment, and that C3 is associated with another whose couplings are small. Note, however, that small couplings need not imply weak binding.

Reduction of C_2H_2 in D_2O by both wild type[42,43] and α-Gln[195] [44] nitrogenases produces predominantly *cis*-CHDCHD**.** Therefore, the C_2H_x fragment being examined must have $x \geq 2$. This is so because loss of a hydrogen upon binding C_2H_2, to form the acetylide (C_2H_1), almost certainly would lead to enzymatic formation of CD_2CHD. To proceed, we incorporated the results of the ^{1}H ENDOR measurements, and examined the various possibilites offered by considering the S_{EPR1} state is associated with a C_2H_x fragment, $x = 2$, 3, or 4. Overall, it seems to us most plausible to suggest that $x = 2$, and that C_2H_2 binds to two Fe atoms in a bridging fashion (formally, as a bridging dianion), as in Figure 4B. Such a structure for bound C_2H_2 explains our ^{1}H ENDOR results in that there is no solvent-derived proton to give rise to the strongly coupled signal. It is also consistent with an earlier proposal[45] of a mechanism for the addition of D atoms to C_2H_2, so as to produce *cis*-CHDCHD. One reasonable possibility is that the D atoms destined to reductively cleave the C−Fe bond also bind to these same Fe atoms, as sketched in Figure 4B.

In summary, Q-band ^{13}C and ^{1}H ENDOR of the S_{EPR1} turnover state of α-Gln[195] MoFe protein formed in the presence of $^{13}C_2H_2$ and of $C_2^{1,2}H_2$ revealed the first direct evidence of the molecular interaction between the FeMo-cofactor and C_2H_2. At least two C_2H_x species are bound to the cofactor of the S_{EPR1} species. We believe the most attractive interpretation of the data is that one of the species is C_2H_2 ($x = 2$) that binds in the bridging mode (Figure 4) to two Fe ions of the FeMo-cofactor, thereby stabilizing the $S = {}^1/_2$ cluster state. Our current results are highly significant in that they represent the first detection and structural identification of an intermediate of C_2H_2 reduction. They encourage us in a search for an altered MoFe protein that exhibits an EPR signal that is specifically associated with the natural substrate, N_2, under turnover conditions. As in the case for C_2H_2 described here, such studies would provide important clues about where and how N_2 becomes bound to FeMo-cofactor during nitrogenase catalysis.

Acknowledgment. This work has been supported by NIH R01-GM59087 (D.R.D.), MCB-9904018 (B.M.H.), and USDA 97-37305-4879 (B.M.H.) and 99-35305-8645 (B.J.H.).

JA000542G

(39) Christiansen, J.; Cash, V. L.; Seefeldt, L. C.; Dean, D. R. *J. Biol. Chem.* **2000**, in press.

(40) Fessenden, R. W.; Schuler, R. H. *J. Chem. Phys.* **1963**, *39*, 2147.

(41) Adrian, F. J.; Cochran, E. L.; Bowers, V. A. *Free Radicals in Inorganic Chemistry*; American Chemical Society: Washington, DC, 1962.

(42) Dilworth, M. J. *Biochim. Biophys. Acta* **1966**, *127*, 285−294.

(43) Hardy, R. W. F.; Holsten, R. D.; Jackson, E. K.; Burns, R. C. *Plant Physiol.* **1968**, *43*, 1185−1207.

(44) Newton, W. E.; Fisher, K.; Kim, C.-H.; Shen, J.; Cantwell, J. S.; Thrasher, K. S.; Dean, D. R. In *Nitrogen Fixation: Fundamentals and Applications*; Tekhenovich, I. A., Provorov, N. A., Romanov, V. I., Newton, W. E., Eds.; Kuwer Academic Publisher: Dordrecht, The Netherlands, 1995; pp 121−127,

(45) Stiefel, E. I. *Proc. Natl. Acad. Sci. U.S.A.* **1973**, *70*, 988−992.